26 May 2010, 4:45 pm - 6:45 pm

Analysis of Soil Nailed Walls Under Harmonic Dynamic Excitations Using Finite Difference Method

Alimohammad Sheikhbahaei
Isfahan University of Technology, Iran

Amir M. Halabian
Isfahan University of Technology, Iran

S. Hamid Hashemolhosseini
Isfahan University of Technology, Iran

Fifth International Conference on
Recent Advances in Geotechnical Earthquake Engineering and Soil Dynamics
and Symposium in Honor of Professor I.M. Idriss
May 24-29, 2010 • San Diego, California

ANALYSIS OF SOIL NAILED WALLS UNDER HARMONIC DYNAMIC EXCITATIONS USING FINITE DIFFERENCE METHOD

Alimohammad Sheikhbahaei
Dept of Civil Eng. Isfahan Univ. of Tech.
Isfahan, Iran

Amir M. Halabian, S. Hamid Hashemolhosseini
Dept of Civil Eng., Dept of Mining Eng., Isfahan Univ. of Tech
Isfahan, Iran

ABSTRACT

Soil nailing is an efficient method to stabilize different soil structures. The method has been extensively used for improving stability of slopes. The construction process of Soil nailed walls commonly involve three basic sections: excavation, nail installation and face stabilization. The nail bars are inserted into ground by either drilling or grouting and are usually arranged in both horizontal and vertical directions. Present research intends to understand Soil-nailed wall behavior under dynamic excitations. Employing finite difference method a three dimensional model has been developed in the proper finite difference code. Soil constitutive behavior for dynamic analyses is predicted taking into account soil hysteresis behavior. To simulate nail bars cable structural elements are employed and also liner structural elements will be utilized for shotcrete facing. Dynamic excitation incorporated as semi-seismic harmonic loading is applied at the bottom of the model where represents soil subgrade. The boundary conditions are considered to be antisymmetric during dynamic analyses. Effects of different crucial factors are monitored during investigations. Some parameters such as, input motion frequency, nail inclination, nail length as well as soil strength properties have been examined.

INTRODUCTION

The use of soil-nailed walls which consists of passive reinforcement of the existing ground by installing closely spaced steel bars or cables encased in grout has gained a lot of popularity in recent years. This method is typically used in order to stabilize slopes and excavations where sequential construction is beneficial in comparison with other common gravity and retaining walls. The process of construction of soil-nailed walls commonly involves three important stages: excavation, nail installation and face stabilization. The fundamental stability concept of soil-nailed walls is based on reinforcing soil mass with reinforcement elements such as steel rebars so that the soil mass would behave as a unit mass. Soil nailed wall systems are well suited to excavation applications where vertical or near-vertical cuts are mandatory. Furthermore, Soil-nailed walls have presented remarkably well performance during many strong motions, unlike the poor performance of common gravity retaining structures.

Slope stability analyses based on limit-force equilibrium methods have been developed to assess the global stability of soil-nailed wall together with local stability of reinforced soil mass by taking into account different factors influencing wall performance, i.e. shearing, tension and pull-out resistance of the inclusions. One of the most common methods used to analyze soil-nailed walls is pseudo-static approach by which dynamic earth pressure is computed using conventional Mononobe-Okabe or a modified two-part wedge method (Okabe, S., 1924). Despite the fact that these methods provide satisfactory information about both overall and internal stability of the structure, they cannot succeed to provide any information regarding mobilized forces along nail bars as well as deformations of the structure. Therefore, due to the fact that these approaches are not sufficient to predict wall behavior, numerical methods are employed in order to have better understanding of wall performance under both static and dynamic loading conditions. Nevertheless there are a few studies concerning dynamic behavior of the soil-nailed walls.

PREVIOUS RELATED WORK

Due to significant flexibility of soil-nailed walls which is attributed to particular construction procedure of these systems, soil nailed walls can experience more deflections comparing with other common gravity walls. After the 1989

Loma Prieta, California; 1995 Kobe, Japan; and 2001 Nisqually, Washington earthquakes, it was reportedly observed that soil nailed walls have shown no sign of being distressed or significant permanent deflection, despite having experienced, in some cases, ground accelerations as high as 0.7g . The observations from post-earthquake investigations imply that soil-nailed walls appear to have an inherent satisfactory seismic response. This has been attributed to the intrinsic flexibility of soil-nailed wall system and possibly some level of conservatism in current design procedures (FHWA, 2003). As a result, these systems are definitely appropriate choice for many geotechnical engineering purposes. The pseudo-static working stress design methods mostly used for seismic evaluation of soil-reinforced systems as well as soil-nailed walls are derived from the pseudo-static Mononobe, Matuso and Okabe modified Coulomb's solution to account for inertia forces corresponding to the estimated earthquake induced horizontal accelerations. There are several methods by which the distribution and magnitude of dynamic forces along reinforcements could be determined. Some of these methods use theoretical and numerical procedures to evaluate structure performance under dynamic loading conditions, but some methods use empirical formulations rather than numerical simulation to evaluate wall performance.
In recent decades, a few researches have been carried out which have considered behavior of soil-nailed walls under dynamic conditions. Most of the current studies are based on pseudo-static limit equilibrium methods (Mononobe-Okabe) in which seismic accelerations are applied to the active wedge of soil mass. However, Limit equilibrium methods fail to give any information regarding developed tensile and shear forces along nail bars and they cannot evaluate local stability of structure. Therefore, Numerically-derived Pseudo-static approaches are developed to investigate behavior of soil-nailed walls under dynamic loading conditions.
Seed et al., 1975 conducted finite element analyses to examine seismic response of reinforced earth retaining walls. They considered an inertia force for the potential active zone which is in proportion with the weight of the active zone. Finally, the proposed method by these investigators incorporated in the FHWA design guidelines for reinforced soil systems.
Dhouib developed a non-linear finite element code to model reinforced soil walls subjected to dynamic loading. The results of investigations indicated that the incremental dynamic force is proportional to the distribution of static forces and the geometry of the active zone under dynamic loading is a function of the earthquake acceleration (Choukeir, 1997).
Segrestin et al., 1988 conducted finite element analyses to understand seismic response of soil-reinforced structures. In their studies the elastoplastic behavior of the soil was simulated by varying the modulus of elasticity as a function of observed deformations. The results of study indicate that the distribution of dynamic tensile forces along the strips is fairly uniform and does not give significant change in the position of points of maximum tension.
Sabahit et al. presented a new pseudo-dynamic method to analyze soil-nailed slopes. By Assuming constant shear modulus and limited shear wave velocity in addition to varying earthquake acceleration along wall depth, they obtained the total required reinforcement forces (Choukeir,1997).
The present paper aims to focus on the seismic behavior of the soil-nailed retaining structures which has shown significant resistance to lateral loadings due to earthquakes. The method used to undertake research is numerical finite difference method. Therefore, a three dimensional finite difference mesh has been developed representing soil medium, along with cable and liner elements to simulate nail bars and shotcrete facing. Having better perception of soil behavior under seismic excitations a nonlinear hysteretic soil constitutive model has been employed. Moreover, the paper outlines the interaction mechanism between different components of soil-nailed walls along with soil constitutive model as well as governing equations to analyze soil-nailed structures. In conclusion, a comprehensive parametric study has been conduct examining effects of crucial parameters on performance of these structures under seismic loading situations.

NUMERICAL SIMULATION

The present research seeks to have better understanding of seismic response of soil-nailed structures. Therefore, a 3-Dimensional model has been developed to gain better perception of soil-nailed structures behavior. In order to simulate different components of soil-nailed walls numerous elements have been employed. It should be noted that the model dimensions has to be determined wide enough so that the effects of boundary conditions on the response of structure would be negligible.
The process of wall construction takes place in five stages. After each stage of excavation, Nail installation and application of shotcrete facing would accomplish. The wall is initially designed for static loading using conventional limit equilibrium methods.
The finite difference mesh used for analyses is illustrated in Fig. 1-a. This mesh employed for analyses is made up of quadrilateral continuum elements which will represent soil medium. While the vectors of nodal forces in each nodal point equate the external forces, the model meets the equilibrium conditions. Thus, the determining factor to monitor model equilibrium would be maximum unbalanced forces. Due to repetitive arrangement of nail bars along the length of the excavation, only a slice of the soil mass between the vertical plane crossing nail centerlines an another vertical plane the mid-point of the adjacent nail bars examined. To have more reliable results of analyses a somewhat finer mesh is utilized for those areas near the excavation face. The construction process is modeled by successive excavation of soil which after each stage the placement of nail bars and then applying shotcrete takes place. In the finite difference code these sequences is established using null model. This feature provides removing an specified area from the model. Likewise it helps to simulate excavation process of a soil-nailed wall i.e. removing soil mass, placement of nail bars and application of shotcrete. It should be noted that initial state of equilibrium

has to be established before any stage proceeds. Afterward as each excavation ends, the equilibrium conditions (according to Maximum unbalanced force) will be examined in order to ensure whether or not that model meets equilibrium conditions to resume next stage. Fig. 1-b exhibits the soil nailed wall in equilibrium conditions after fifth stage of excavation.

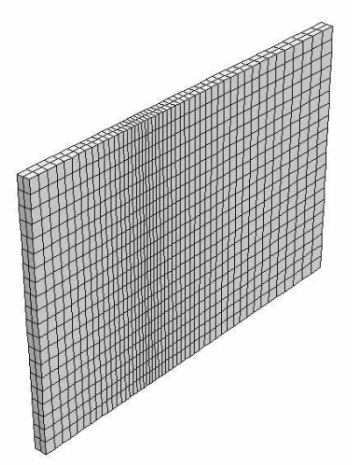

(a)

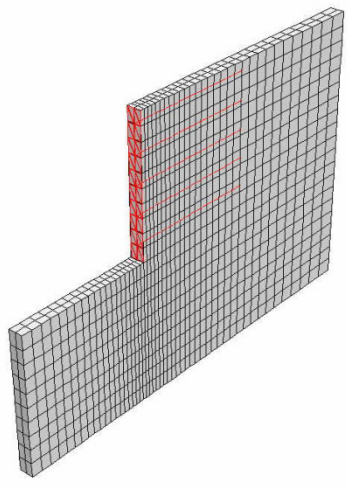

(b)

Fig. 1 – a) Finite difference mesh used for analyses – b) Soil nailed wall after fifth stage of excavation

SOIL CONSTITUTIVE MODEL

The failure criterion for the soil used in dynamic analyses is the Mohr-Coulomb shear failure criterion together with a non-linear hysteretic constitutive behavior under cyclic loading conditions.

For most of complex simulations in dynamic loading conditions, the soil shear behavior can be predicted using non-linear cyclic relationships. For instance, in many studies Masing rule has been implemented to simulate granular soil hysteretic constitutive behavior during which unloading reloading relationship will be followed.

In contrast to equivalent linear methods, non-linearity introduced by the constitutive behavior of soil leads the governing dynamic equilibrium equations to be reduced to the incremental form. Therefore, only one computational run is accomplished with a fully nonlinear method, since the nonlinearity in the stress-strain law is followed directly by each element. Providing an appropriate law, the dependence of damping and shear modulus on strain level are modeled automatically.

Despite requiring more computational efforts by employing this approach the use of different constitutive models could be studied conveniently. An accurate non-linear dynamic soil-structure interaction problem requires an efficient solving algorithm as well as a nonlinear soil constitutive law that also captures the hysteretic behavior of soil during loading and reloading phases of transient loads to represent energy-absorbing characteristics of soil material. FLAC3D, 1996 is a numerical computer program widely used in geotechnical engineering based on explicit finite difference scheme. The non-linear soil model adapted in the program can correctly represent the physics of the actual soil; however, it requires more parameters to define the soil behavior. This may be resulted from not being adequately user friendly from structural engineer's point of view. If hysteretic-type model is used and no extra damping is specified, then the damping and tangent modulus are appropriate to the level of excitation at each point in time and space, since these parameters are embodied in the constitutive model. In this study, the elastic behavior of soil in the model ground is assumed to demonstrate the hysteretic characteristics based on the hyperbolic model for stress-strain relationships. Fig. 2 shows the typical hysteretic curve on the $\tau - \gamma$ relationships (Ishihara, 1996). The skeleton curve is given by the following hyperbolic equation:

$$\tau = \frac{G_o}{1 + \gamma/\gamma_o}\gamma \qquad (1)$$

As seen in Fig. 1, G_o is the shear modulus at the initial part of the backbone curve and γ_r is the reference strain defined as;

$$\gamma_r = \frac{\tau_f}{G} \qquad (2)$$

where τ_f is the soil shear strength (horizontal asymptote at large strains) and τ and γ are given as follows:

$$\tau = \sigma_1 - \sigma_3 \; ; \gamma = \varepsilon_1 - \varepsilon_3 \qquad (3)$$

G_O can be obtained by Hardin-Dernevich relation (Prakash 1981):

$$G_o = \alpha \frac{(2.973 - e)^2}{1 + e} \cdot \left(\frac{1 + 2k_o}{3}\right)^{1/2} \cdot \sqrt{\sigma_v'} \qquad (4)$$

in which e, σ_v', K_o and are void ratio, effective vertical stress and confining pressure ratio, respectively.

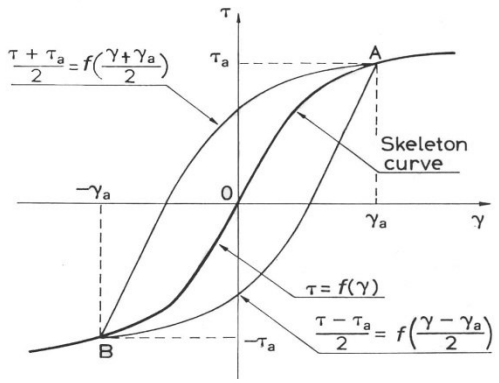

Fig. 2. Soil stress-strain relationship

The sign of the γ increment, $d\gamma$, judges the reversal of loading direction. For each loading-reloading loop, after reversal point, the unloading path is defined as;

$$\frac{\tau - \tau_a}{2} = f\left(\frac{\gamma - \gamma_a}{2}\right) \tag{5}$$

in which τ_a and γ_a are the shear stress and shear strain at the reversal point. In the hyperbolic model the tangent shear modulus of elasticity for loading and reloading can be obtained from:

$$G_t = \begin{cases} \dfrac{G_{max}}{\left[1-(\frac{G_{max}}{\tau_{max}})|\gamma|\right]^2} & for\ loading \\ \dfrac{G_{max}}{\left[1-(\frac{G_{max}}{2\tau_{max}})|\gamma-\gamma_\varepsilon|\right]^2} & for\ reloading \end{cases} \tag{6}$$

In this study, an energy dissipation approach was used to predict the reversal point in loading-reloading paths of hysteretic loop. Based on this approach the reversal loading direction is judged by the sign of the dissipated energy increment (the incremental shear work), ΔWS. The shear work increment can be obtained in a FEM analysis as the different between the total incremental work, ΔWT, and the incremental volumetric work, ΔWN, for an increment strain during loading or reloading as

$$\Delta W_s = \Delta W_T - \Delta W_N \tag{7}$$

where

$$\Delta W_T = \sigma_{11}\Delta\varepsilon_{11} + \sigma_{22}\Delta\varepsilon_{22} + \sigma_{33}\Delta\varepsilon_{33} + 2(\sigma_{12}\Delta\varepsilon_{12} + \sigma_{13}\Delta\varepsilon_{13} + \sigma_{23}\Delta\varepsilon_{23}) \tag{8}$$

$$\Delta W_N = \frac{1}{3} \cdot \sum_{k=1}^{k=3} \sigma_{kk}\, \Delta\varepsilon_{\mathrm{kk}} \tag{9}$$

The rebound shear modulus can be calculated by effective stresses through a non-linear dynamic analysis. This basic model can produce curves of apparent damping and modulus versus cyclic strain that resemble results from laboratory tests (Fig. 3).

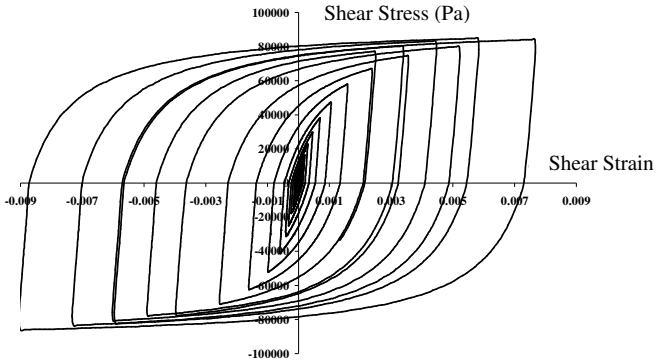

Fig.3 - Cyclic shear stress-shear strain curve for an element in FE model

In the plastic zone the Mohr-Coulomb failure constitutive model was adopted where the failure envelope corresponds to Mohr-Coulomb criteria. According to this theory, failure along a plane in the soil occurs by a critical combination of normal and shear stresses and not by normal or shear stress alone. The functional relation between normal and shear stress on the failure, generally referred to as the Mohr-Coulomb criteria, can be given by a failure envelope defined as

$$\tau_f = c' + \sigma'_{nf} tan\varphi' \tag{10}$$

where τ_f and σ'_{nf} are the shear and normal effective stresses on the failure plane, c' is cohesion and φ' is the drained angle of shearing resistance. Variation of shear stress with shear strain using Mohr-Coulomb yield criterion along with nonlinear hysteretic behavior under cyclic loading conditions is depicted in Fig. 4. The Mohr-Coulomb is assumed to be perfectly plastic. Therefore, there is no hardening/softening criterion required (Halabian, A.M, et al. 2008). Using the Mohr-Coulomb criteria, the yield function can be defined as:

$$F(\{\sigma'\},\{k\}) = \sigma_1 - \sigma_3 - 2c'cos\varphi' + (\sigma_1 + \sigma_3)sin\varphi' \tag{11}$$

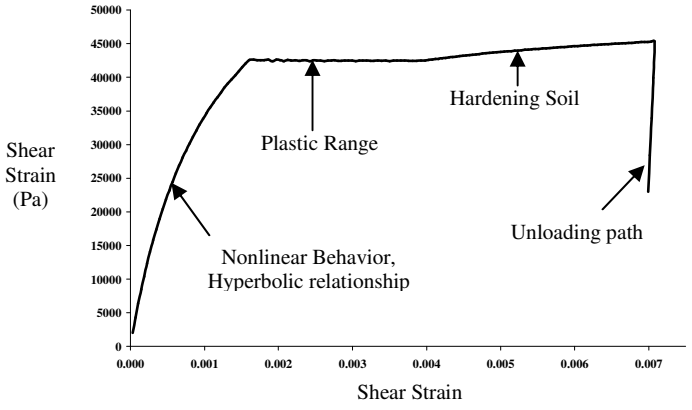

Fig. 4 - Variation of shear stress with shear strain (Mohr-Coulomb yield criterion with nonlinear behavior)

SOIL NAILS MODELING

As indicated earlier, Cable structural elements have been employed to simulate soil nails (Fig. 5). A one-dimensional constitutive model is adequate for describing the axial behavior of the reinforcing member. The axial stiffness K is determined based on the reinforcement cross-sectional area A, Young's modulus E and CableSEL length L by the relation

$$K = \frac{AE}{L} \tag{12}$$

A tensile and compressive-yield strength, F_t and F_c, may be assigned to the CableSEL such that cable forces cannot develop that are greater than these limits. (Fig. 6)

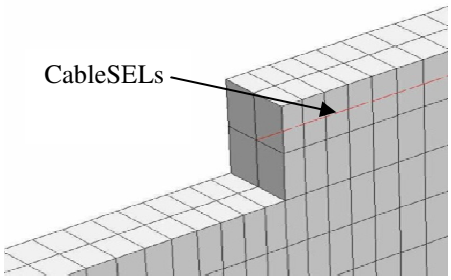

Fig. 5 - CableSEL elements used for soil-nails modeling

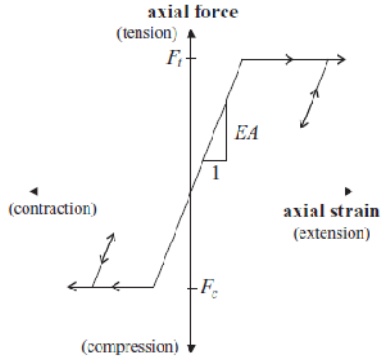

Fig. 6 - Cable material behavior for CableSELs

The most general method to determine properties for fully bonded soil-nail behavior is to conduct pull-out tests on small segments of grouted nail in the field. Typically it has been assumed that segments with 50 cm length are grouted into boreholes and the end of these segments are pulled with a jack mounted to the surface of the tunnel and attached to cable via a barrel and wedge-type anchor (Fig. 7). Then the force applied to nail is plotted against deformation of the nail. Consequently the grout shear stiffness is obtained through calculating slope of this curve. Therefore according to pull-out test results grout shear stiffness assumed to be $7 \times 10^3 \frac{\text{kN}}{\text{m}}/\text{m}$. The nail parameters are presented in Table 1.

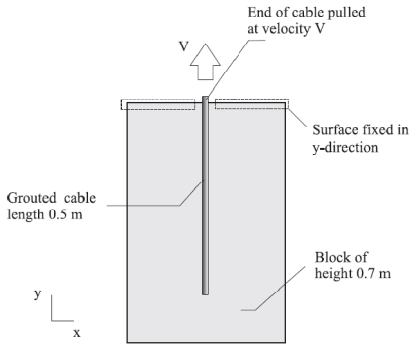

Fig. 7. Schematic view of pull-out test model

SOIL-NAIL INTERFACE MODELING

The shear behavior of cable-soil interface is naturally cohesive and frictional. This system is represented as a spring-slider system which is placed at each nodal point along the cable axis [Fig. 8 (a)]. The shear behavior of the grout annulus, during relative shear displacement between the cable/grout interface and the grout/soil interface, as illustrated in Fig. 8 (b) , is described numerically by; the grout shear stiffness kg; the grout cohesive strength c_g; the grout friction angle φ_g; the grout exposed perimeter pg; and the effective confining stress σ_m. Fig. 9. (a),(b) depicts a typical scheme of the grouted cable mechanical behavior. (FLAC3D, 1996)

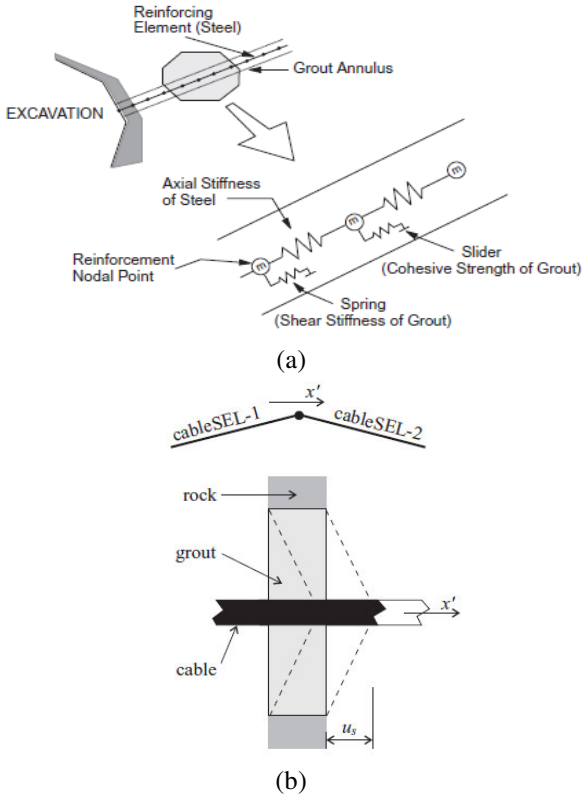

Fig. 8 - a) Mechanical representation of fully bonded reinforcement - b) Idealization of grouted-cable system

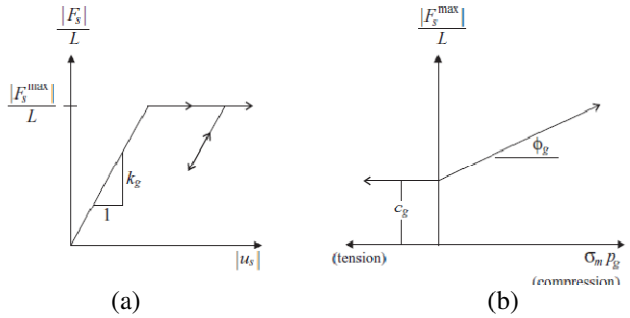

(a) (b)

Fig. 9 - Grout material behavior for CableSEL s, a) shear force/length versus relative shear displacement, us b) shear-strength criterion

The effective confining stress σm would act in the plane perpendicular to the cable axis, and is calculated at each nodal point along the cable axis, based on the stress acting in the zone to which the nodal point is connected. Denote the cable-axis direction as x', and denote the principal stresses acting in the y'z' -plane as σ_1 and σ_1, such that $\sigma_1 > \sigma_2$ (tension positive). Then the value of σ_m is taken as

$$\sigma_m = -\left(\frac{\sigma_1 + \sigma_2}{2} + p\right) \qquad (13)$$

To compute the relative displacement at the cable-soil interface, an interpolation scheme is employed to estimate the displacement of the soil in the cable axial direction at each cable node, based on the displacement field in the zone to which the node is connected.

FACING MODELING

Liner Structural Elements has also been incorporated to represent shotcrete made wall facing of soil-nailed walls (Fig. 10). In order to simulate a wall facing a collection of LinerSEL elements are employed. The mechanical behavior of each LinerSEL element can be divided into the structural response of the liner material itself and the way in which the LinerSEL interacts with the FLAC3D grid. Liners are used in order to simulate thin liners, for instance soil-nailed wall facings, for which both normal-directed compressive/tensile interaction and shear-directed frictional interaction with the host medium occurs (FLAC3D, 1996). The properties of the facing wall were assigned the following values: Elastic Modulus, $E = 25$ GPa ; Poisson Ratio,$\upsilon = 0.2$; Unit Weight, $\gamma = 24\ \mathrm{kN/m^3}$.

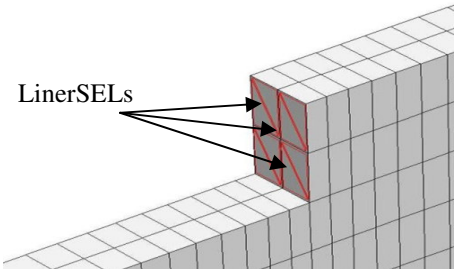

Fig. 10 - LinerSEL elements used for facing modeling

SOIL-FACING INTERFACE MODELING

The interface behavior is represented numerically at each liner node by a linear spring with finite tensile strength in the normal direction and a spring-slider in the tangent plane to the liner surface. The orientation of the spring-slider changes in response to relative shear displacement us between the liner and the host medium, as shown in Fig. 11.

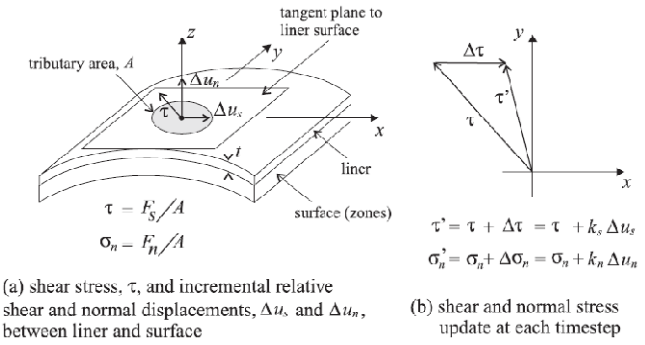

(a) shear stress, τ, and incremental relative shear and normal displacements, Δu_s and Δu_n, between liner and surface

(b) shear and normal stress update at each timestep

Fig. 11 - Idealization of Interface behavior along liner surface

HARMONIC BASE EXCITATIONS

As cited earlier, the numerical model was excited at the foundation elevation by a variable-amplitude harmonic motion with a frequency close to the fundamental frequency of the reference structure. Despite having a single frequency content and short duration of excitation, this variable-amplitude harmonic ground motion has a satisfactory similarity with that of actual earthquake acceleration so that the results of analyses appears to be helpful to understand the effects of crucial parameters on the performance of soil-nailed structure under actual earthquake acceleration records. Although, the analyses of soil-nailed structures under actual earthquake motions will include some extent of complexity and are considered to be time-consuming runs.

However, after static equilibrium was achieved, the full width of the foundation was subjected to the variable-amplitude harmonic ground motion record illustrated in Fig. 12. This acceleration record was applied horizontally to all nodes at the bottom of the soil zone. The accelerogram follows a trend which has both increasing and decaying peak acceleration parts and will be expressed as below;

$$\ddot{U}(t) = \frac{1}{2}\left(1 - \cos\left(\frac{2\pi}{T}t\right)\right)\sin(2\pi f t) \qquad (14)$$

where; t=time, T=duration of net harmonic excitation, f=frequency. In order to specify other properties of harmonic ground motion a free-field analysis of soil-nailed structure has been carried out. Subsequently, the value of typical input motion frequency has been chosen close to fundamental frequency of system (2 Hz) and the peak amplitude of the harmonic base excitation is equal to 0.1g. Specifications used for soil medium in the analyses are presented in Table 1.

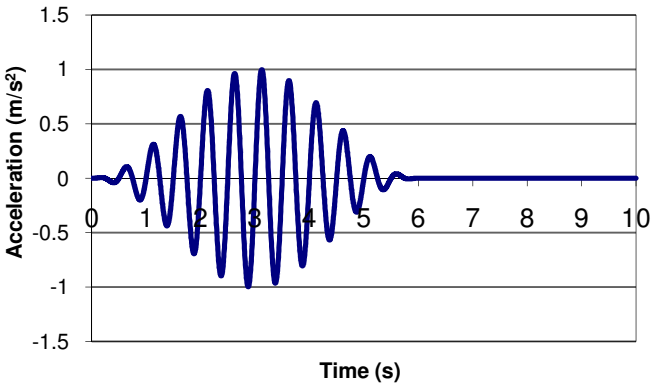

Fig. 12 - Base reference excitation history

Table 1 – Soil and Nail Characteristics used for harmonic wave base excitations analyses

Characteristics	**Soil**	Nail
E (MPa)	50	200
Poison Ratio, υ	0.25	-
Tensile Strength (MPa)	-	460
Friction Angle, φ^o	28	-
Cohesion, C (kPa)	5	-
Density, ρ (kg/m^3)	1900	7800
Dilation Angle, ψ^o	1	-
Shear Modulus, G_{max} (kPa)	60	-
Length (m)	-	9
Radius (m)	-	0.025

GOVERNING EQUATIONS AND SOLUTION

As it was mention previously, the method which was employed to perform analyses has been finite different method. Thereby, mechanics of each continuum can be derived from main principles, i.e. definition of strain motion, motion laws together with constitutive equations defining the material as an idealized system. Equation of motion and equilibrium governing on an unbounded medium is expressed as following:

$$\sigma_{i,j} + \rho b_i = \rho \frac{dv_i}{dt} \quad i,j = 1,2,3 \qquad (15)$$

where ρ is the mass per unit volume of the medium, b_i is the body force per unit mass, and $\frac{dv_i}{dt}$ is the material derivative of the velocity. In the Finite difference method, these governing equations represent the motion of an elementary volume of the medium subjected to the forces. Constitutive law usually comes in form of following equation:

$$\breve{\sigma}_{ij} = H_{ij}(\sigma_{ij}, \varepsilon_{ij}, \kappa) \qquad (16)$$

which $[\breve{\sigma}_{ij}]$ is the co-rotational stress-rate tensor H_{ij} is the given function related to Mohr-Coulomb yield criterion, κ is a parameter which takes into account the history of loading, while ε_{ij} is a strain rate tensor

Figure 6 displays the flow diagram of the computational cycle incorporated in a finite difference formulation. To solve the governing equations, an explicit "time-marching" finite difference solution scheme is used. For each timestep the calculation sequence can be summarized as below:

1. New strain rates are derived from nodal velocities
2. Constitutive equations are used to calculate new stresses from the strain rates and stresses at the previous time.
3. The equation of motion is invoked in order to derive new nodal velocities and displacements from stresses and forces.

The sequence is repeated at every timestep, and the maximum unbalanced (out-of-balance) force in the model is monitored. This force will either approach zero indicating that system has reached equilibrium conditions or it will approach a constant (i.e. non-zero value) pointing that a portion of the model is in a steady-state (plastic) flow of material. This trend is an explicit calculation approach and each complete cycle in this trend is recognized as a timestep. (FLAC3D, 1996)

For static or steady state solution, the rate of kinetic energy in the model should reach a negligible value. This purpose is achieved through damping the equations of motion. At the end of the static solution process, the model will be either at an equilibrium state or at steady flow state which a part of the model (or somewhat the entire model) is failed (i.e. unstable) under the applied loading conditions. To determine whether the model undergoes instability of encounters the equilibrium, the maximum nodal force vector referred as unbalanced force is used as the convergence parameter.

Generally, there are two approaches by which dynamic analyses are conducted; Equivalent Linear Approach, Fully Non-linear Approach. The method used in the present study to conduct dynamic analyses is a fully nonlinear method in which only one run is done while the soil nonlinearity in the stress-strain is followed directly by each element as the solution marches on in time. Using appropriate nonlinearity the dependence of damping and apparent modulus on strain level is modeled. However there are various nonlinear models built in FLAC3D program intending primarily for use in quasi-static loading or in dynamic conditions where the response is mainly monotonic. Thereby, a good model for

dynamic soil-structure interaction would capture the hysteresis curves and energy absorbing characteristics for real soil. The materials herein were used for soil backfill are more likely to be granular material which possess nonlinear behavior with hysteresis energy dissipation when they are subjected to cyclic loading. Using the hysteresis model implemented in the dynamic analyses helps to better simulate soil nonlinearity of backfill soil.

After static equilibrium is achieved the full width of soil subgrade is subjected to Harmonic wave excitations. Several additional base excitations were used to examine the influence of the reference harmonic base input acceleration function on wall response. Anti-symmetric boundary conditions were used in order to undertake dynamic analyses. Having better simulation of boundaries during numerical dynamic analyses the boundary conditions at the sides of the model must account for the free-field motion that would exist in the absence of the structure. Therefore, a Free-field boundary conditions were used at the left and right edges of the model to permit for the radiation of the elastic waves to the far field. The base condition is freed in the horizontal direction while the soil subgrade is subjected to horizontal harmonic excitations.

RESULTS OF DYNAMIC ANALYSES

Influence of the frequency of Input harmonic motion

The influence of frequency of Input harmonic acceleration record on the results of numerical simulations were investigated by carrying out a series of analyses with an input frequency f=2, 4, 6 and 8 Hz. Example horizontal displacement histories at the crest of the wall for numerical analyses is presented in Fig. 13. The displacement histories indicate that the horizontal displacement at the crest of the wall were influenced by the input ground harmonic motion frequency and increase monotonically with time during the harmonic base excitation. However, with regard to the results of a series of analyses with different input motion frequencies, it can be concluded that increase in input motion frequencies will result in reduction of horizontal displacement at the wall crest.

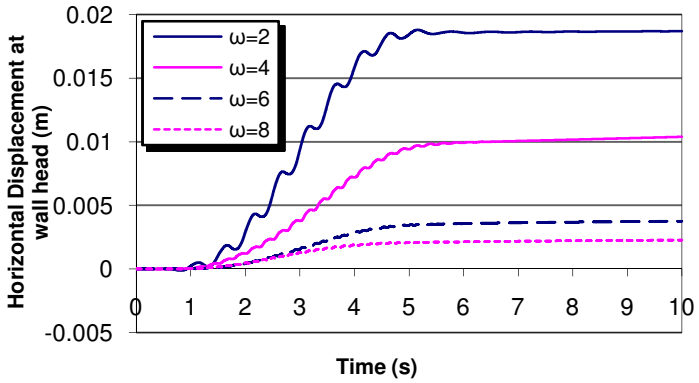

Fig. 13 – Horizontal displacement response time history at the wall head during the harmonic base excitation

Fig. 14 indicates that while the input frequency motion increases the peak outward horizontal displacement of the wall decrease.

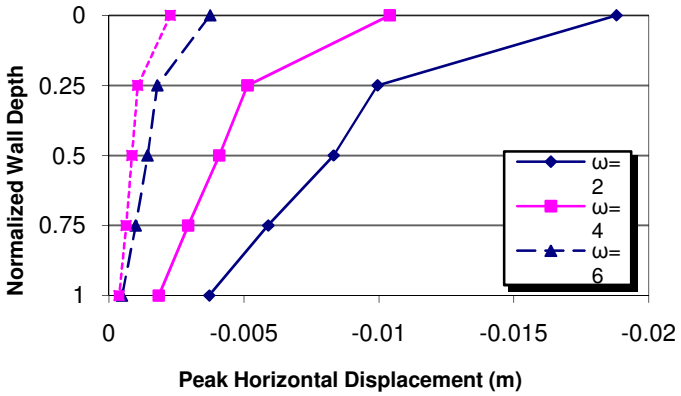

Fig. 14 - Normalized peak horizontal displacement distribution along height of wall facing

Conversely, as illustrated by Fig. 15 the peak horizontal acceleration response along the wall facing has increased by an ascending trend of input motion frequency.

It was found by further studies that as the input motion frequency approaches fundamental frequency of the system, the structure will demonstrate more critical responses.

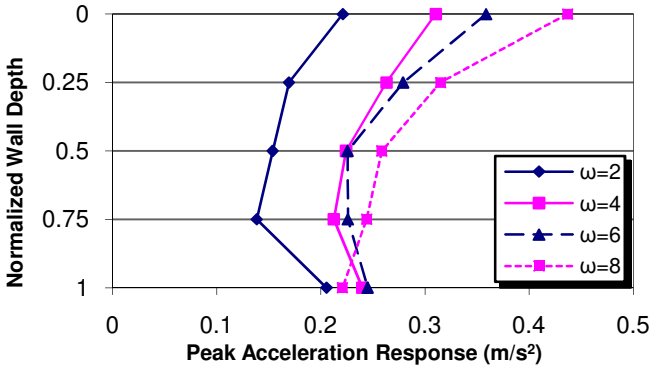

Fig. 15- Normalized peak horizontal acceleration along height of wall facing

As illustrated in Fig. 16, it is worth noting that increasing input motion frequency made tensile forces to less mobilize along nail bars due to the fact that the critical state becomes more inaccessible since the input frequency motion gets further from fundamental frequency of the system.

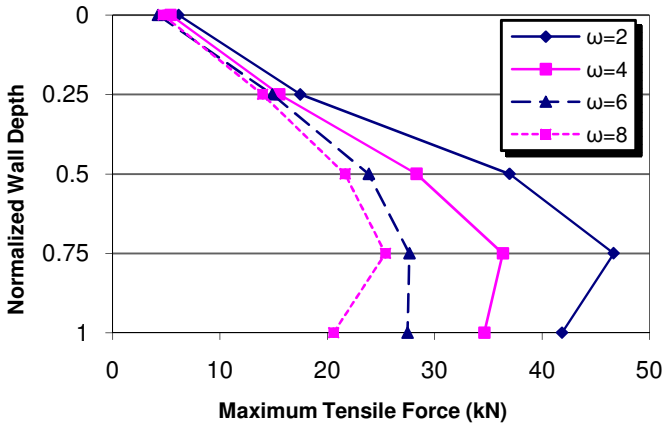

Fig. 16 - Maximum tensile forces distribution along height of wall facing

Influence of angle of nail inclination

The influence of nail inclination angle on dynamic response of the structure was examined using models with four different nail inclination angles. Fig 17 shows that the magnitude of the horizontal displacement at the crest of the wall decrease as the nail inclination angle increases. However, it was observed that the improving effect of increasing nail inclination angle on reduction of wall horizontal displacements is not permanent. As shown in Fig. 18, the peak outward horizontal displacement of the wall show decrease in value by increasing nail inclination angle while it varies in the range of 0^o to 15^o. Afterward, increasing nail inclination angle results in slight increase of wall deformations. The increase in wall deformation would be more substantial as it ranges in $25^o - 30^o$. As a result, it was shown that the increase in nail inclination angle would have destabilizing effect on the performance of structure during harmonic base excitations.

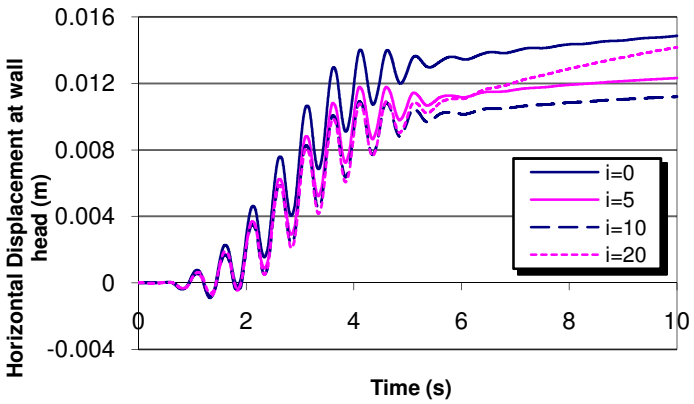

Fig. 17 - Horizontal displacement response time history at the wall head during the harmonic base excitation

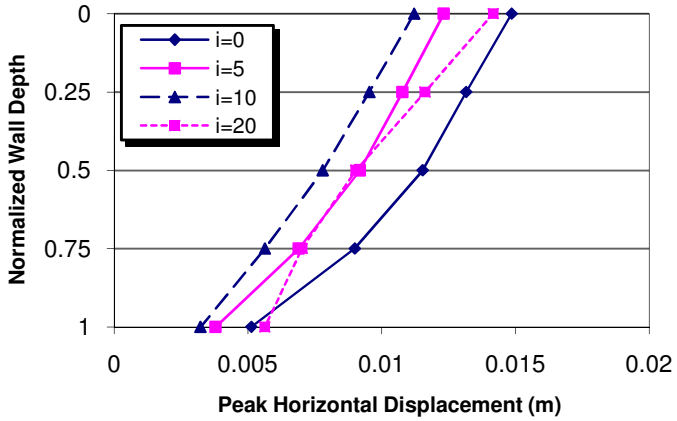

Fig. 18 - Normalized peak horizontal displacement distribution along height of wall facing

Fig. 19 shows variations of peak horizontal acceleration response along the wall facing with nail inclination angle. As illustrated, it can be concluded that increasing nail inclination angle would result in increase of peak horizontal acceleration response of the wall. Fig. 20 shows distribution of maximum tensile forces along nail bars. It is of interest to note that tensile forces along nail bars increases for the four upper nail bars as their inclination angle increases.

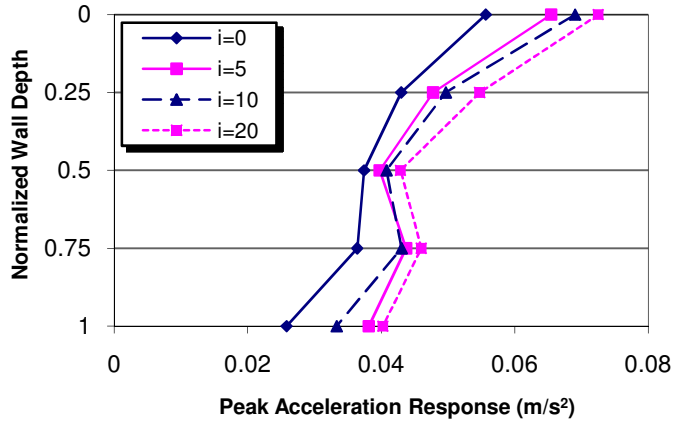

Fig. 19 - Normalized peak horizontal acceleration along height of wall facing

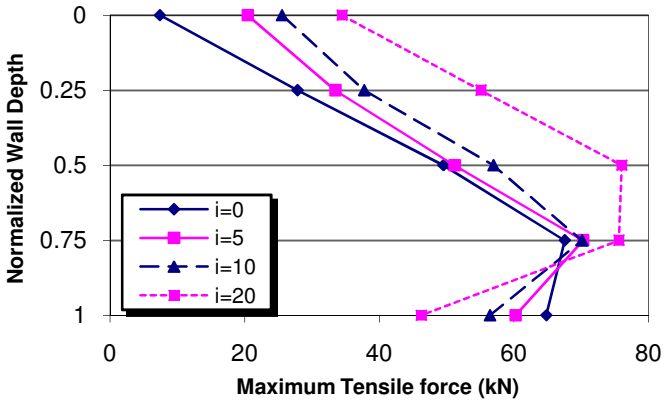

Fig. 20 - Maximum tensile forces distribution along height of wall facing

Influence of nail length

The influence of nail length on dynamic response of the structure was studied using models with four different nail lengths. It can be observed from Fig. 21 that lengthening the nail bars would result in reduction of wall horizontal displacement at the wall crest.

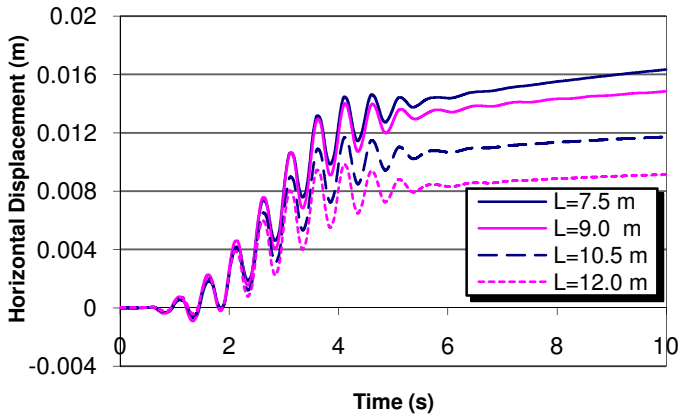

Fig. 21 - Horizontal displacement response time history at the wall head during the harmonic base excitation

Moreover, as shown in Fig. 22, the peak outward horizontal displacement of the wall decreases as the nails length increases.

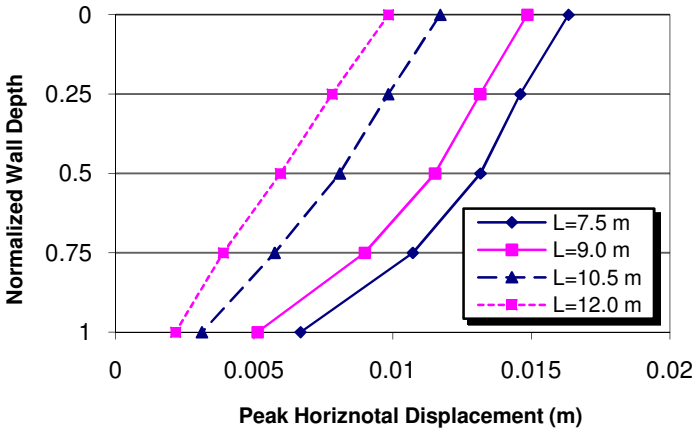

Fig. 22 - Normalized peak horizontal displacement distribution along height of wall facing

The variations of peak horizontal acceleration response along the wall facing with nail length are summarized in Fig. 23. The peak horizontal acceleration along the wall facing has been greater for longer nail bars. However the major influence of nail length on increasing the peak horizontal acceleration response of the wall would be in the range of 7.5 m to 10 m. Therefore, there would be no considerable influence as the nail length increases beyond the value of 12 m.

Fig. 24 illustrates the distribution of maximum tensile forces along nail bars with variations of nails length. The results indicate that there would not be significant difference in the mobilized maximum tensile forces along nail bars (excluding the third nail) as the nails length increases.

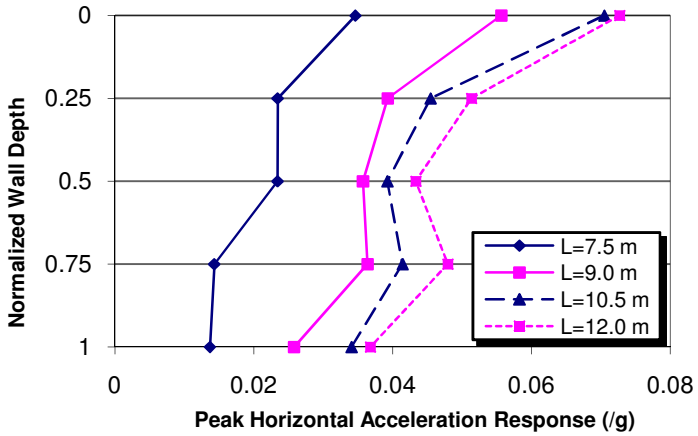

Fig. 23 - Normalized peak horizontal acceleration along height of wall facing

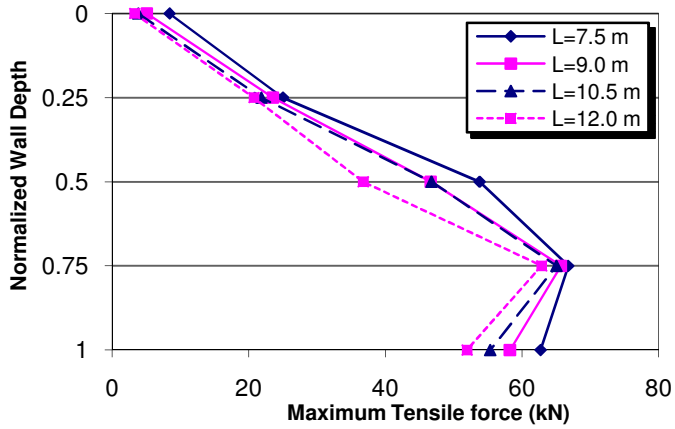

Fig. 24 - Maximum tensile forces distribution along height of wall facing

Influence of soil strength properties

The effects of soil strength properties on the wall performance are investigated based on peak horizontal displacement along the wall facing and the maximum mobilized tensile forces along the nail bars. As to the results of analyses it can be concluded that increasing in soil strength properties would improve soil shear strength so that soil-nailed wall would better resist against dynamic loads due to harmonic base excitation. As illustrated in Fig. 25 and 26, peak horizontal displacement along wall facing decrease as the soil cohesion and internal friction angle increase. Fig. 27 and 28 show that increasing soil strength properties would result in reduction of maximum tensile forces along nail bars.

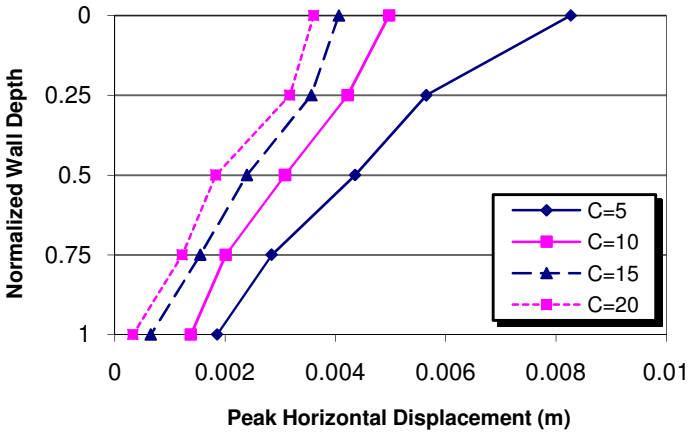

Fig. 25 - Normalized peak horizontal displacement distribution along height of wall facing

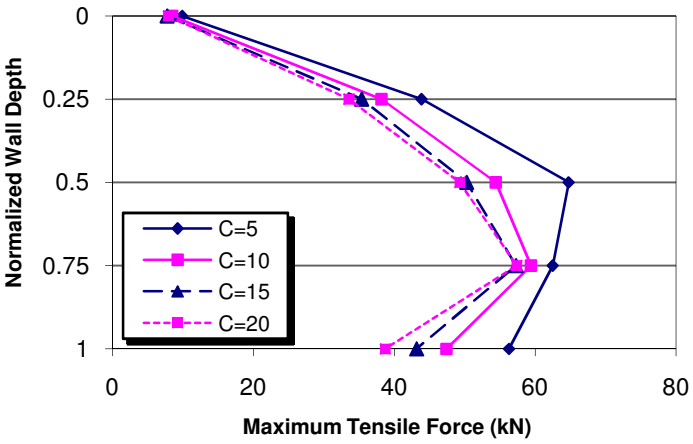

Fig. 26 - Maximum tensile forces distribution along height of wall facing

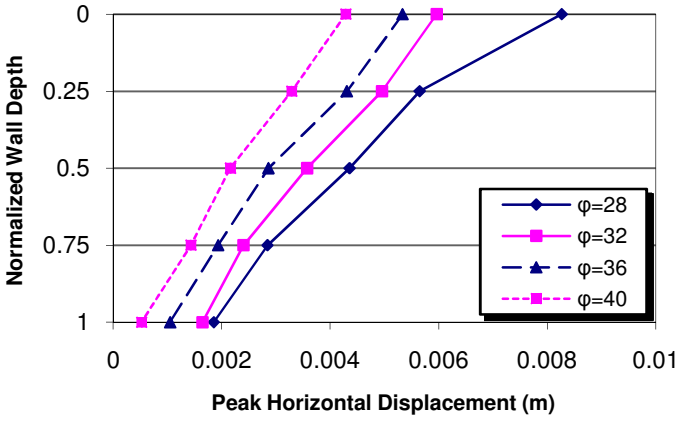

Fig. 27 - Normalized peak horizontal displacement distribution along height of wall facing

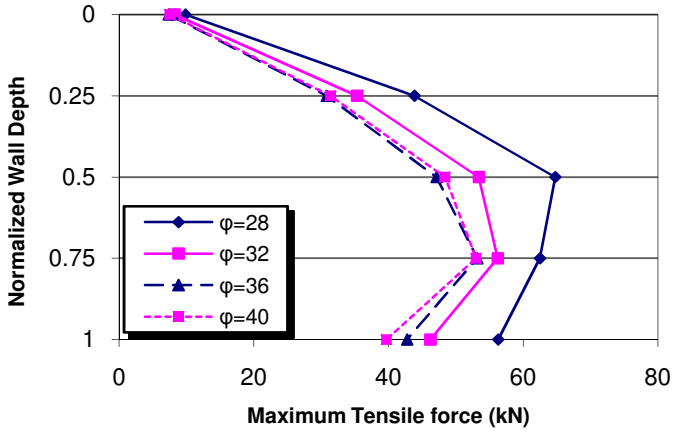

Fig. 28 - Maximum tensile forces distribution along height of wall facing

CONCLUSION

The paper has focused on numerical analysis of 9 m high soil-nailed wall subjected to harmonic base excitations taking into consideration of soil nonlinear hysteresis behavior in order to explore the influence of key parameters such as; input motion frequency, nail inclination angle, nail length and soil strength properties. To simulate the soil medium, nail bars and shotcrete facing, quadrilateral continuum elements along with CableSEL and LinerSEL elements were used respectively. The interaction behavior among different components of structure was simulated carefully in order to have more accurate response of structure. Conducting a comprehensive parametric study, the results of analyses highlight the influence of crucial parameters on performance of soil-nailed walls after being subjected to harmonic base excitations. Some specific important conclusions and discussion points in this regard are summarized as below:

- Horizontal displacement at the wall crest, peak horizontal displacement along the wall facing and maximum tensile force along nail bars decreased as the input motion frequency increased. However, Peak horizontal acceleration response along the wall facing increased by input motion frequency increasing.
- Horizontal displacement at the crest of the wall decrease as the nail inclination angle increases. The peak outward horizontal displacement of the wall show decrease in value by increasing nail inclination angle while it varies in the range of 0^o to 15^o. Increasing nail inclination angle to the values beyond 15^o results in slight increase of wall deformations. The increase in wall deformation would be more substantial as it ranges in $25^o - 30^o$.
- The peak horizontal acceleration response along the wall facing has been greater for lengthy nail bars.
- To enhance the soil strength properties would improve soil shear strength so that soil-nailed wall

would better resist against dynamic loads due to harmonic base excitation.

REFERENCES

Choukeir, M., et al. [1997], "Seismic Design of Reinforced- Earth and Soil- Nailed Structures", *Ground Improvement*, Vol. 1, pp. 223- 238.

FHWA, [2003], "*Geotechnical Engineering Circular No. 7*, *Soil Nail Walls*", Federal Highway Administration (FHWA), Report No. FHWA0-IF-03-017. (Carlos A. Lazarte, Victor Elias, R. David Espinoza, Paul J. Sabatini) Washington, DC., USA.

FLAC3D, [1996], *"Fast Lagrangian Analysis of Continua in 3 Dimensions",* Version 2.10, Itasca Consulting group, Inc., 708 South Third Street, Minneapolis, Minneapolis, USA

Halabian, A.M, et al. [2008], "Seismic response of structures with underground stories considering nonlinear Soil-structure interaction", *Proc. 6th international conference on Case Histories in Geotechnical Engineering*, Arlingtion, VA.

Ishihara,K., [1996], *"Soil Behaviour in Earthquake Engineering"*, Clarendon Press,Oxford University, New York, USA, 350 p.

Okabe, S., [1924], "General Theory on Earth Pressure and Seismic Stability of Retaining Wall andDam",*DobokuGakkaishi - Journal of the Japan Society of Civil Engineers*, Vol. 10, No. 6, pp. 1277-1323. (Translated from Japanese)

Prakash, S. [1981], "*Soil Dynamics"*. McGraw-Hill, Inc.

Seed, H. B., et al. [1975], "*The Generation and Dissipation of Pore Water Pressures During Soil Liquefaction,*" UC-Berkeley, Earthquake Engineering Research Center, NSF Report PB-252 648.

Segrestin, P., and Bastick, M.J. [1988]. "Seismic design of reinforced earth retaining walls". *Proc. International Geotechnical Symposium on Theory and Practice of Earth Reinforcement*, Fukuok Kyushu, Japan, pp. 577–582.